Bull. Mater. Sci., Vol. 33, No. 5, October 2010, pp. 625–632. © Indian Academy of Sciences.

Effect of carbon on mechanical properties of powder-processed Fe–0·35%P alloys

SHEFALI TRIVEDI*, YASHWANT MEHTA, K CHANDRA and P S MISHRA
Indian Institute of Technology, Roorkee 247 667, India

MS received 17 March 2009; revised 18 April 2009

Abstract. **The present paper records the results of mechanical tests on iron-phosphorus powder alloys which were made using a hot powder forging technique. In this process mild steel encapsulated powders were hot forged into slabs, hot rolled and annealed to relieve the residual stresses. These alloys were characterized in terms of microstructure, porosity content/densification, hardness and tensile properties. Densification as high as 98·9% of theoretical density, has been realized. Microstructures of these alloys consist of single-phase ferrite only. Alloys containing 0·35 wt% P, such as Fe–0·35P–2Cu–2Ni–1Si–0·5Mo and Fe–0·35P–2Cu–2Ni–1Si–0·5Mo–0·15C show very high strength. It was observed in this present investigation that, the alloying additions, such as Si, Mo, Ni, and C to Fe–P based alloys caused increase in strength along with reduction in ductility. Cu reduces porosity of Fe–P alloys. Alloys developed in the present investigation were capable of hot working to very thin gauge of sheets and wires.**

Keywords. **Fe–P alloys; mechanical properties; powder metallurgy; forged; ancient iron.**

1. Introduction

Archeological iron is often seen to contain levels of phosphorus which are much higher than those found in modern steels. It produces 'cold short' behaviour or brittleness during cold working (Goodway and Fisher 1988; Rostoker and Bronson 1990; Wiemer 1993). Phosphorus does not, however, render the iron 'hot short or brittle' at high temperature (Percy 1864; Wiemer 1993), so the manufacture in the past of an artifact from phosphoric iron by forging should have posed no problems.

Phosphorus has a marked solid solution strengthening effect in ferrite which is of the same order as the interstitial elements, carbon and nitrogen (Allen 1963; Tylecote 1986; Clarke and McIvor 1989). It produced marked work hardening in iron when cold worked (Tylecote 1986; Wiemer 1993). The increase in flow stress due to the action of phosphorus promotes cleavage fracture thus increasing the likelihood of brittle failure in wrought route (Weng and Mcmahon 1987). Phosphorus also reduces grain boundary cohesion, thus promoting intergranular failure. It is found that the embrittling effect of phosphorus is reduced by the presence of carbon in very small amount (Allen 1963). Phosphorus increases the yield stress and ultimate tensile stress but reduces the elongation and reduction in area at failure, both conventional measures of ductility (Dieter 1988).

In wrought metallurgy, phosphorus is treated as an impurity because in cast steels, phosphorus exhibits strong segregation during solidification, with the formation of inclusions at grain boundaries which lead to embrittlement. Because of this, in the majority of steels its amount does not exceed 0·05%. Cases where certain properties of steels and cast irons improved by higher phosphorus contents are extremely rare (Lindskog and Carlson 1972). The main advantages of phosphorus as an alloying element in powder metallurgy are: its ability to form with metals eutectics of relatively low melting points (970, 1150, 1300 and 1048 for the Cu–P, Ni–P, Co–P and Fe–P systems, respectively) characterized by good fluidity and adhesion to metals and many refractory compounds; high diffusional mobility of its atoms in metals; and its ability to precipitation-harden metals and at comparatively low cost (Muchnik 1977).

Near full density pure Fe P/M parts can be very easily manufactured using conventional powder metallurgical process. It was observed that partial replacement of silicon by a small amount of phosphorus will activate sintering process in Fe–Si alloys by the formation of low melting eutectic phase with iron. Copper in Fe–P alloy helps to reduce porosity. Molybdenum, nickel alloying element, improves strength of Fe–P alloy. Small amount of carbon is helpful to drive out phosphorus from grain boundaries. Phosphorus also helps carrying alloy constituents into iron matrix which are otherwise sluggish to diffuse. Phosphorus significantly improves ductility and strength of Fe–P based powder alloys (Koczac and

*Author for correspondence (shefalitrivedi2k8@gmail.com)

Aggarwal 1978–1979). It is, therefore, realized that, the Fe–P based alloys, containing alloying elements, such as silicon, molybdenum, nickel could be used for structural application because of their higher strength than pure iron with reasonably good ductility. Since all these alloying elements (except nickel) are ferrite stabilizers, ferrite phase will be stable even at high temperature when substantial alloying is completed. Self-diffusion coefficient of iron (Qu *et al* 1991) and inter-diffusion coefficient of the alloying elements in ferrite is much higher than that in austenite. This diffusion helps in reducing amount of pores in the P/M part. However, during alloying process some additional pores may be created (Qu *et al* 1991) (due to dissolution of elemental particles).

If we follow the traditional powder metallurgical process, such as compaction and sintering, for manufacturing high phosphorus Fe–P based alloys, heavy volume shrinkage will be experienced (Moyer 1998). There are several other densification processes available in the literature. Out of all densification processes available, hot iso-static pressing (HIP) is the best as far as density and performance of these P/M parts are concerned. However, the process is extremely costly. Therefore, some pseudo HIP processing could be used for manufacturing these alloys to reduce the cost of processing without sacrificing the benefit of HIP processing. However, HIP process does not have scope of cleaning particle surfaces during processing. Furthermore, existence of prior particle boundaries (PPB) renders them unsuitable because PPBs are sources of impurity concentration resulting in inter-particle brittle failure.

In view of this, in the present investigation, densification of the Fe–P based alloys was carried out by hot powder forging (Chandra 2002) technique. Volume shrinkage associated with these alloys is also no more a consideration in hot powder forging. Hot powder forging has another feature which is not available with compacting in a die or HIP. It is essentially the process where shaping and consolidation are deformation based. This causes redistribution of residual impurities if any, situated at the particle surfaces and renders improvement in properties of the final product (Das 2008).

2. Experimental

For making Fe–P–Cu–Mo–Ni–Si (with or without carbon) alloys by powder metallurgical technique, ferro-phosphorus, ferro-silicon and ferro-molybdenum powders were prepared separately by grinding lumps of ferro-phosphorus, ferro-silicon and ferro-molybdenum (containing 22% P, 70% Si, 60% Mo, respectively) with the help of mortar and pestle (iron) or filing. Powders with –200 mesh size were employed for preparation of alloys. Pure copper and nickel powders having –200 mesh sizes were taken for preparation of these alloys. The powder blends were manually mixed to make desired alloy chemistry. About 500 g of each blended mixture was then poured into a mild steel capsule (as shown in figure 1). The encapsulated powders were heated in a tubular furnace at 1150°C for 45 min in dry hydrogen atmosphere in order to remove the oxide layer from the surfaces of the powder particles. Heated capsules were then forged with a 200T capacity friction screw press to make slabs using a channel die. Two P/M alloys were made in the present investigation. These are: (a) Fe–0·35 wt% P–2 wt% Cu–2 wt% Ni–1 wt% Si–0·5 wt% Mo alloy and (b) Fe–0·35 wt% P–2 wt% Cu–2 wt% Ni–1 wt% Si–0·5 wt% Mo–0·15 wt% C alloy.

The compositions of these alloys are based on the powder mixture. Figure 2 schematically illustrates the process of making slabs through hot powder forging technique. The slabs were then homogenized at 1350°C for 2–3 h depending on the alloy composition to eliminate compositional inhomogeneity. Silicon containing alloys were heated for 3 h whereas alloys without silicon content were heated for 2 h. This is because diffusion of silicon in iron is much slower than the other alloying elements.

All the alloying elements are present in the form of fine particles around pure iron particles. This iron particle is 100% gamma-phase at the homogenizing temperature. Phosphorus (in the form of ferro-phosphorus) combines with this gamma iron powder particle and dissolves in it. As it dissolves, it gets converted into ferrite (figures 3 and 4) and as ferrite phase grows out of gamma phase, more and more phosphorus penetrates into it. This helps carry all the other alloying elements in ferrite phase with the exception of carbon. This is because carbon has very low solubility in ferrite. Consequently carbon is pushed towards gamma rich region (Erhart and Grabke 1981). As the homogenization proceeds, clear partitioning of alloying elements between ferrite and gamma iron takes place. At the end of homogenization, a major portion of carbon segregates in gamma iron region whereas the other alloying elements are concentrated in the ferrite region. After completion of homogenization and lowering of temperatures during furnace cooling there is no gamma phase left as per the equilibrium phase diagram. Carbon diffuses interstitially on cooling, into ferrite, thereby ensuring complete distribution of all the alloying elements including carbon.

Mild steel encapsulation was then removed by machining. The slabs, after removal of mild steel skin, were hot rolled using flat roll and section roll at 900°C to make thin sheets and wires, respectively. Rolling was carried out very slowly at 900°C with 0·1 mm thickness/diameter reduction per pass. The rolling was done using small laboratory scale rolling mill with 10 cm roll diameter. The sheets and wires were then vacuum annealed at 950°C for 40 min to relieve the residual stresses. All the samples prepared this way were characterized in terms of

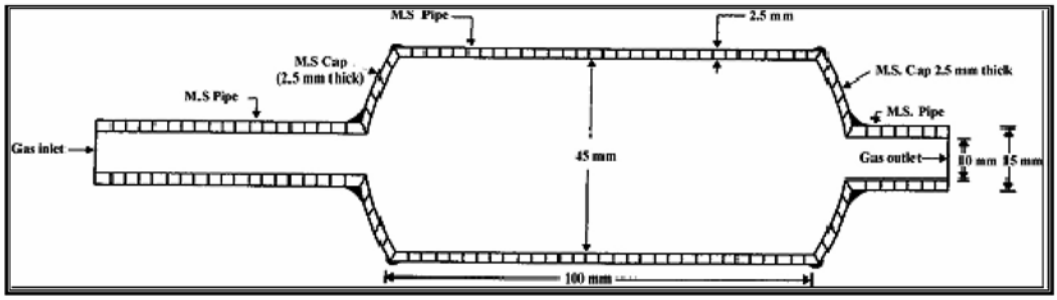

Figure 1. Cross-section of mild steel capsule used in the present investigation.

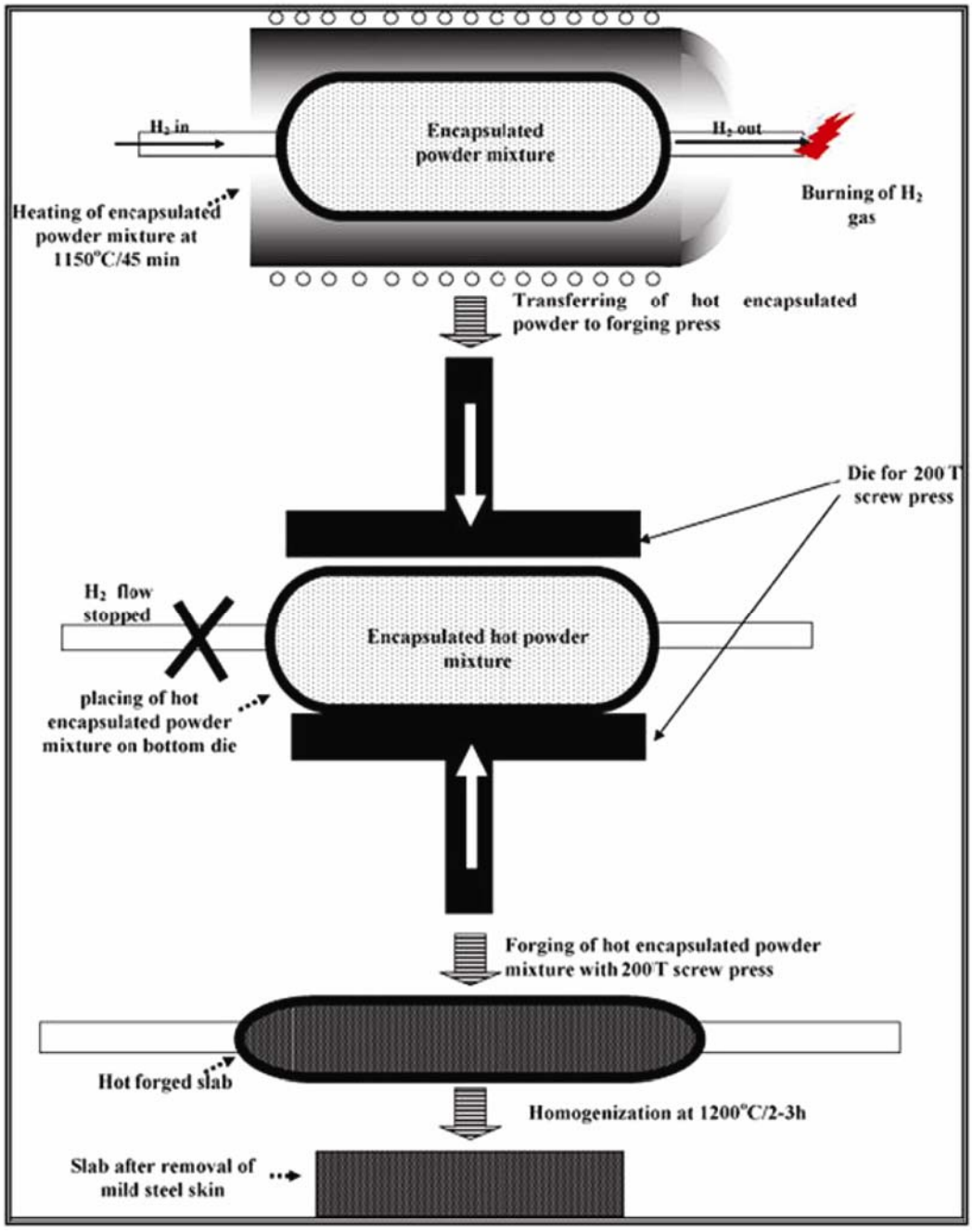

Figure 2. Schematic diagram illustrating the production of slab by hot forging of encapsulated powder mixture.

Table 1. Chemical composition of Fe–P alloys (wt%).

Sample	P	Ni	Cu	Si	Mo	C	Fe
(a)	0·35	2·0	2·0	1·0	0·5	–	Balance
(b)	0·35	2·0	2·0	1·0	0·5	0·15	Balance

Table 2. Calculated volume percentage of porosities of the alloys (homogenized at 1350°C).

Sample no.	As forged density (g/cc)	Rolled and annealed density (g/cc)	Theoretical density (g/cc)	Porosity in rolled and annealed wires, calculated using measured density (Vol. %)	Porosity in rolled and annealed wires, calculated using quantitative metallographic technique (Vol. %)
(a)	7·166	7·524	7·648	1·62	2·25
(b)	7·50	7·510	7·620	1·44	2·00

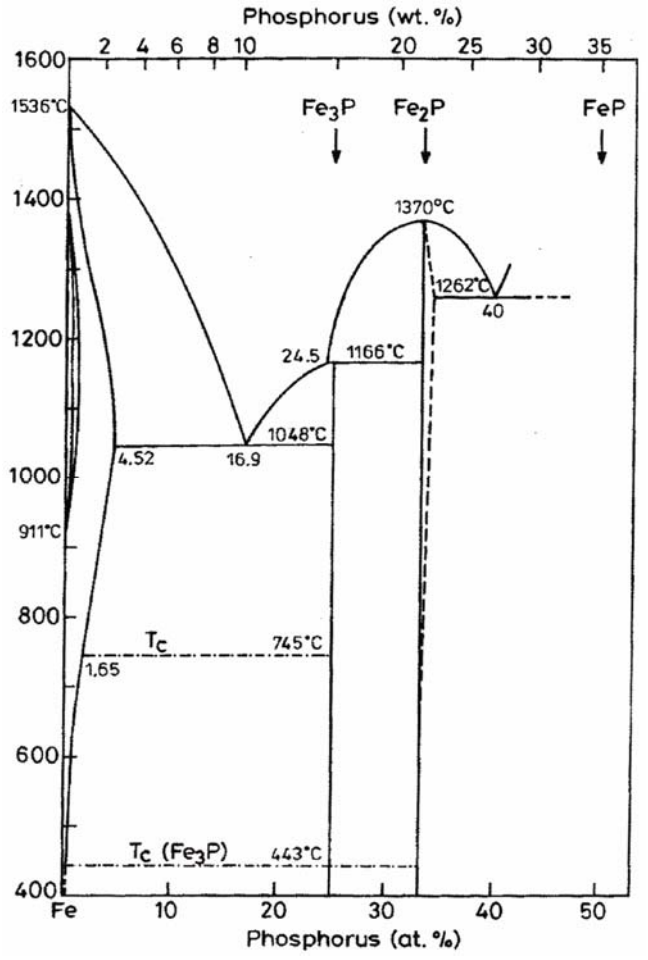

Figure 3. Fe–P binary phase diagram (Kubaschewski 1982).

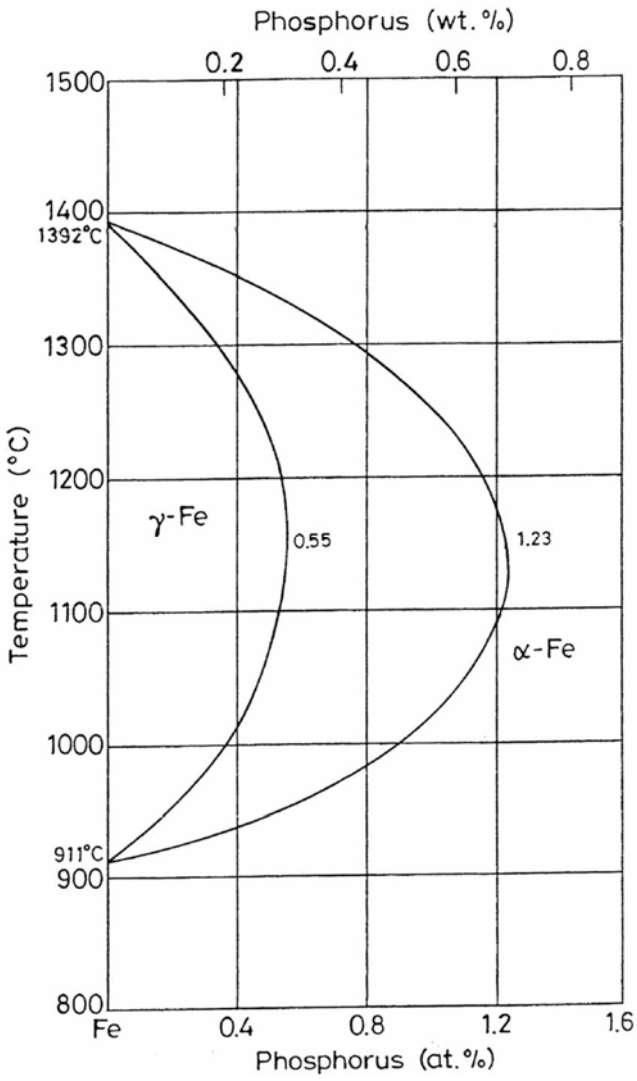

Figure 4. High temperature gamma loop region of the Fe–P phase diagram (Kubaschewski 1982).

density, microstructure, hardness, and tensile properties as detailed below.

Homogenized slabs as well as hot rolled and annealed sheets and wires were subjected to metallographic examinations for determining calculated porosity shown in table 2. This includes volume percentage of porosity and grain size. Calculated volume percentage porosities matched with the volume percentage porosities measured by the metallographic method. Hardness of the hot rolled and annealed wires were measured with Vicker's hard-

ness tester using 10 kg load. Samples for tensile testing were either punched out of sheet or wires. The tensile specimens were tested using Hounsfield tensile tester. The tensile testing was carried out at room temperature with a cross head speed of 1 mm/min. Gauge length of the specimens was 20 mm. Gauge diameter of the tensile sample (wires) was 1 mm.

3. Results and discussion

Chemical compositions of Fe–P alloys in weight percentage are shown in table 1. Volume percentage porosities were estimated from the measured density of the specimens. These estimated volume percentage of porosities are recorded in table 2. In order to verify the correctness of the estimated volume percentage of porosity, the porosities were also measured using quantitative metallographic technique. Rolled and annealed microstructures with the experimentally measured volume percentage of porosity were recorded and shown in figure 5. They are more or less matching with the theoretically calculated volume percentage porosity.

Theoretical density is calculated on the basis of the rule of mixtures, but when the constituents diffuse amongst each other and alloy, some micro-porosity is expected. During processing (hot rolling), oxides also form which lower the density of the product. Such micro-pores and oxides do not help in improving density as they remain in the system irrespective of deformation based processing. Due to the aforesaid reasons we are unable to exceed 98·9% of the estimated theoretical density.

The cross-section of the wires showed almost rounded porosity. It is found that copper helps to reduce the

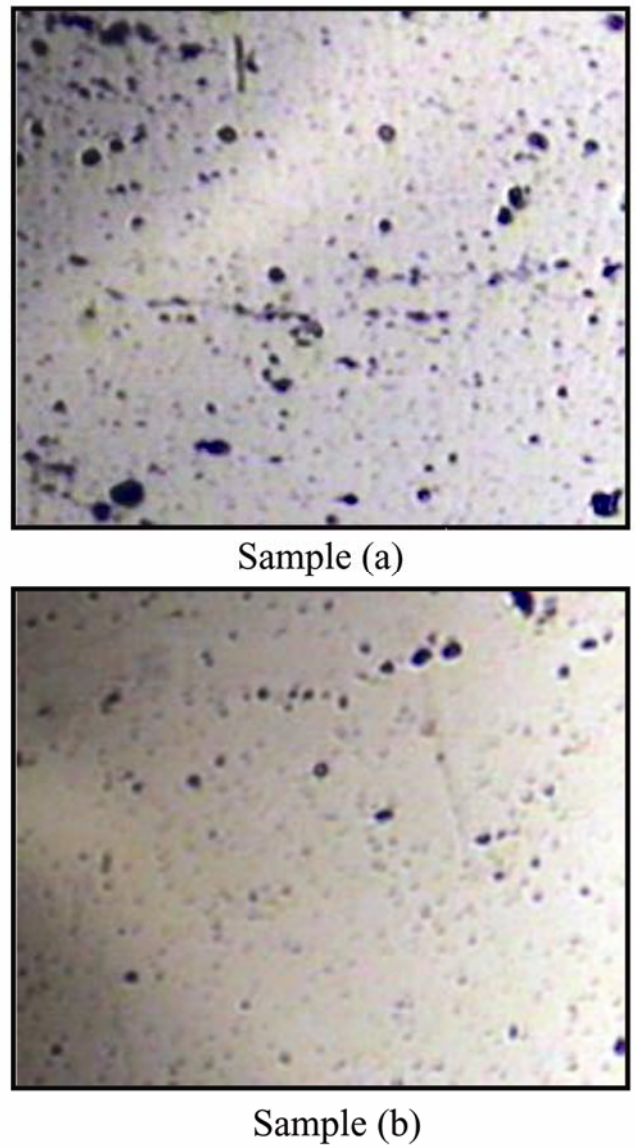

Figure 5. Porosity distribution of the rolled and annealed wires in as polished and unetched condition (homogenized at 1350°C) (Magnification, 100X).

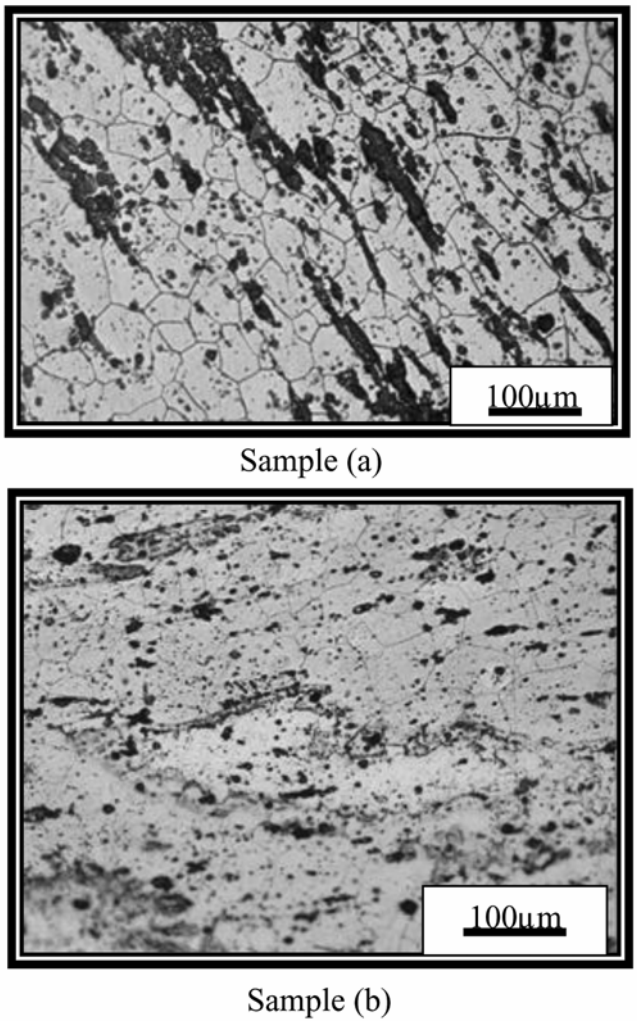

Figure 6. Cross-section of hot rolled and annealed alloys (etched with 2% nital) revealing grain structure. Residual alignment of porosity and flattening of pores are observed in all these rolled and annealed alloys (homogenized at 1350°C).

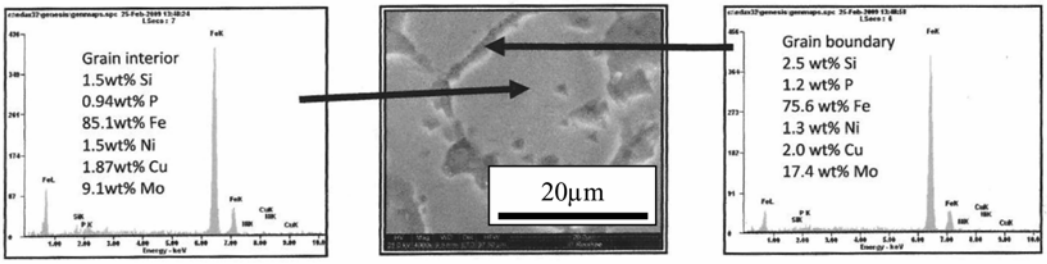

Figure 7. Surface morphology and EDAX pattern from different spots on sample a.

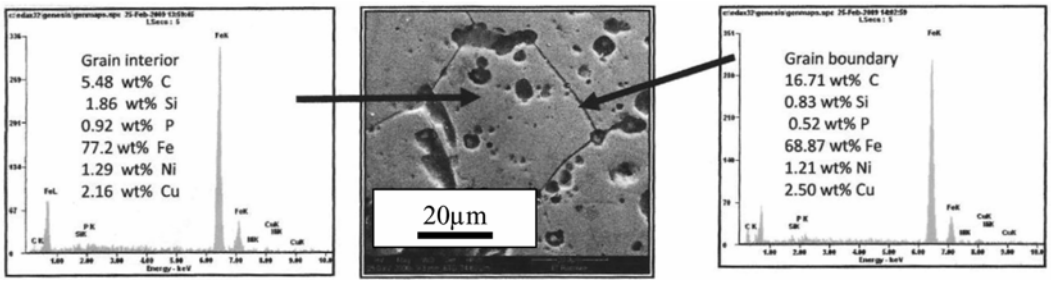

Figure 8. Surface morphology and EDAX pattern from different spots on sample b.

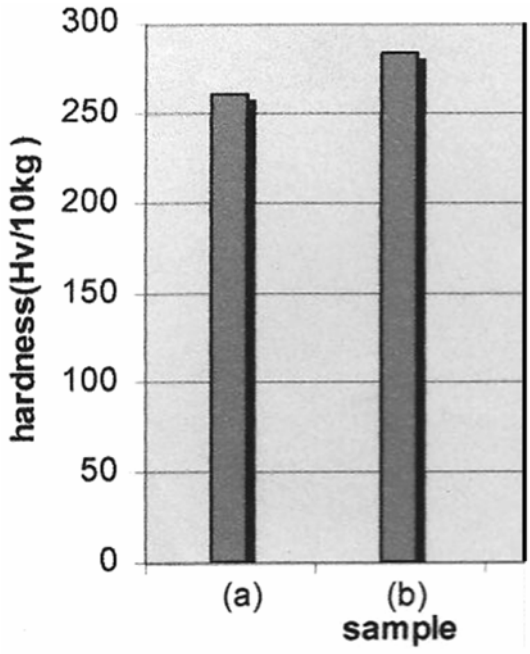

Figure 9. Variation in hardness of P/M alloys (a) and (b).

Table 3. Tensile test of P/M alloys (homogenized at 1350°C).

Sample	Proof stress (MPa)	UTS (MPa)	Total elongation (%)
(a)	254	575	15
(b)	406	815	11·8

volume percentage of porosity in our samples. Further, the pores are predominantly present in the grain interior as is observed in the microstructures which is beneficial for mechanical properties. Cross-sections of wires were etched to reveal grain boundaries and are shown in figure 6. The strength of sample (b) was much higher than that of sample (a). The reason for this can be found in the literature. Carbon displaces phosphorus from the grain boundaries by a site competition effect (Suzuki *et al* 1985; Erhart and Grabke 1986). This causes a reduction in the embrittling effect of phosphorus. Figures 7 and 8 confirm site competition between carbon and phosphorus in our samples.

In general, samples containing silicon, molybdenum, and nickel showed large grains. This may be due to high homogenizing time and temperature used for facilitating effective silicon diffusion. The hardness was found to increase with phosphorus, molybdenum and nickel as well as silicon alloying additions. Figure 9 shows the hardness of different P/M alloys made in this investigation. However, porosity also affected the hardness of these products. The alloy Fe–0·35P–2Ni–2Cu–1Si–0·5Mo having 2·25 vol.% porosity and Fe–0·35P–2Ni–2Cu–1Si–0·5Mo–0·15C with 2·00 vol.% porosity showed considerable improvement in hardness. Their hardness values are 260 Hv/10 kg and 283 Hv/10 kg, respectively. Had there been similar porosity levels in both of these alloys, improvement in hardness due to carbon addition in alloy (b) could have been ascertained.

The Fe–P based alloys containing other alloying elements (Mo, Ni, Si, C, and Cu) show fairly high strength

as compared to alloy (a). Tensile properties, such as proof strength, tensile strength, % elongation of these alloys are shown in table 3.

Figures 10 and 11 show engineering stress–strain curves of the samples (a and b). The reported percentage elongation values have been calculated by the formula:

[(gauge length after fracture – original gauge length)/ (original gauge length)] × 100%,

original gauge length = 15 mm.

The values obtained from the stress–strain curves are slightly higher than the calculated percentage elongation values.

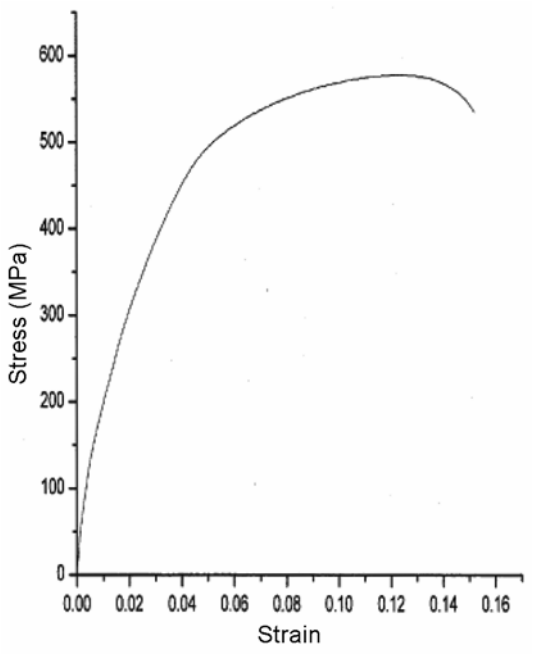

Figure 10. Engineering stress–strain curve of sample (a).

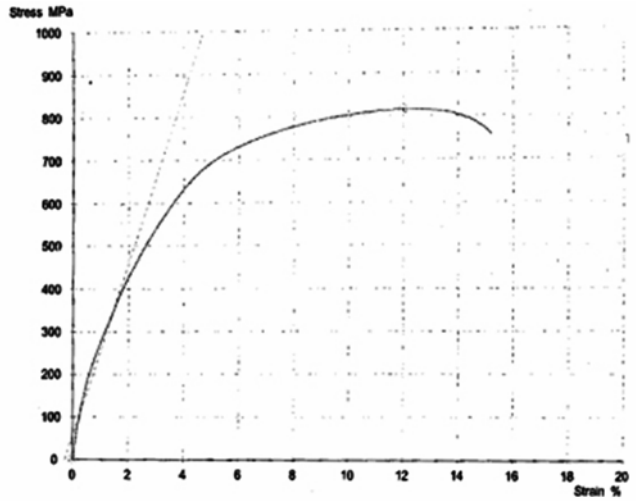

Figure 11. Engineering stress–strain curve of sample (b).

The mechanical properties obtained in the present investigation are suitable for structural applications. Few limited tensile tests under cold deformed conditions exhibited UTS well over 900 MPa. However, ductility came lower marginally. This is possible on account of development of finer grain structures due to cold working.

4. Conclusions

The following conclusions can be drawn from the present investigation:

(I) Alloys developed in the present investigation have very good hot/cold workability.

(II) Alloys containing Mo, Ni, Cu and Si (with or without carbon) showed higher strength (> 575 MPa) and higher resilience value with moderate ductility under annealed conditions with scope for developing higher strengths by cold working.

(III) As forged and homogenized as well as rolled and annealed Fe–P based alloys developed in the present investigation were characterized using metallographic technique. All the microstructures showed single-phase ferrite grains with porosities well distributed along the grain boundaries as well as inside the grains.

(IV) Carbon improved the strength without any high reduction in ductility of sample (b) as compared to sample (a).

(V) Improvement in hardness levels due to the combined addition of carbon with phosphorus was found to be comparatively better than that of alloys (a).

References

Allen N P 1963 *Iron and its dilute solid solutions* (New York: Wiley Interscience) pp 271–308

Chandra K 2002 *Development of iron-P based soft magnetic materials by P/M route*, Ph D Thesis, Indian Institute of Technology, Roorkee

Clarke B D and McIvor I D 1989 *Ironmaking Steelmaking* **16** 335

Das J, Chandra K, Misra P S and Sarma B 2008 *Mater. Sci. & Eng.* **A479** 164

Dieter G E 1988 *Mechanical metallurgy* (London: McGraw-Hill) 3rd edn

Erhart H and Grabke H J 1981 *Met. Sci.* **15** 401

Goodway M and Fisher R M 1988 *Hist. Metall.* **22** 21

Kubaschewski O 1982 *Iron—Binary phase diagrams* (Berlin: Springer Verlag) pp 84–86

Koczac M J and Aggarwal P 1978–1979 *Prog. Powder Metall.* **34–35** 113

Lindskog P and Carlson A 1972 *Powder Metall. Int.* **39** 4

Moyer K H 1998 *ASM Handbook on powder metallurgy and application* **Vol. 7**, p. 1006

Muchnik S V 1977 *Phosphorus-containing alloys, Encyclopedia of inorganic materials* (in Russian) Vol. 2 US Kiev pp 666

Percy J 1864 *Metallurgy—iron and steel* (London: John Murray)

Qu X, Gowri S and Lund J A 1991 *Int. J. Powder Metall.* **27** 9

Rostoker W and Bronson B 1990 *Pre-industrial iron–its technology and ethnology Archeomaterials Monograph No. 1* (Philadelphia PA: University of Pennsylvania)

Suzuki S, Abiko K and Kimura H 1985 *Trans. ISIJ* **25** 62

Tylecote R E 1986 *The prehistory of metallurgy in the British isles* (London: The Institute of Metals)

Weng Y Q and Mcmahon C J 1987 *Mater. Sci. Technol.* **3** 207

Wiemer K 1993 *Early British iron edged tools – A metallurgical survey*, Ph D Thesis, University of Cambridge, Cambridge